ISSN 0036-0236, Russian Journal of Inorganic Chemistry, 2008, Vol. 53, No. 4, pp. 539–544. © Pleiades Publishing, Ltd., 2008.
Original Russian Text © L.A. Elshina, V.Ya. Kudyakov, V.B. Malkov, N.G. Molchanova, 2008, published in Zhurnal Neorganicheskoi Khimii, 2008, Vol. 53, No. 4, pp. 594–600.

Creation of Thin Oxide Coatings and Oxide Nanopowders by Anodic Oxidation of Metals in Molten Salts

L. A. Elshina, V. Ya. Kudyakov, V. B. Malkov, and N. G. Molchanova

Institute of High-Temperature Electrochemistry, Ural Division, Russian Academy of Sciences, Yekaterinburg, Russia

Received December 15, 2006

Abstract—We studied the feasibility of synthesizing ultrafine oxide powders by anodic oxidation of metals, such as zirconium and tantalum, in chloride + nitrate melts at temperatures above 830 K. We showed that, varying the electrolyte composition, oxidation temperature, and anodic current density, one obtains either compact protective coatings on the specified metals or oxide powders with particle sizes of 50 to 200 nm.

DOI: 10.1134/S0036023608040098

Manufacturing of thin oxide films on metals and oxide powders with ultrafine grain sizes and associated high specific surface areas is an important problem of materials science. Several processes exist for manufacturing such powders with set grain sizes, including electrochemical ones. However, the implementation of these processes either is difficult or requires high power supply or additional stages (the preparation of precursors and the separation of final products). Several studies concerned the manufacture of oxide nanopowders from molten salts [1, 2]. But the processes described there can only be implemented in an electrical discharge; moreover, they only produce very small amounts of oxide nanopowders or require some complicated preliminary operations, such as oxychloride synthesis.

In this context, a good alternative to the aforementioned methods is the direct one-pot synthesis of thin oxide films and oxide nanopowders by reacting metals that have high oxygen affinities with chloride melts doped with an oxygen-containing anion, in particular, nitrate anion.

This work studies whether it is feasible to prepare tantalum pentoxide and zirconia with particle sizes within 70 nm and to create thin oxide films by oxidation of zirconium and tantalum in cesium chloride + sodium chloride eutectic melts containing 0.1 to 30 wt % sodium nitrate under an argon atmosphere. Metal oxidation in oxygen-containing aqueous solutions or salt melts remains one of the simplest and efficient methods for synthesizing oxides on the surfaces of various metal products and billets. Multiple studies in this field demonstrated that protection against atmospheric corrosion was provided by surface passivation and high-temperature oxidation.

EXPERIMENTAL

We chose to study zirconium and tantalum for their rather high oxygen affinities and high thermal stabilities and for a high demand in zirconia (the major component for the synthesis of the electrolyte for solid oxide fuel cells) and in tantalum pentoxide (for manufacturing condensers with high specific capacities). Iodide zirconium (99.99%) and tantalum (99.00%) were used in oxidation. Zirconium and tantalum samples were in the form of cylinders with surface areas of ~3.5 cm^2. The electrolyte was prepared from chemically pure salts. Experiments were carried out in a three-electrode high-temperature quartz cell with an encapsulated silver/silver chloride reference electrode, which was connected to a working electrode through a porous asbestos screen; a platinum wire was an auxiliary electrode. A fused and finely ground cesium chloride + sodium chloride eutectic mixture with 0.1–30 wt % sodium nitrate (chemically pure grade) was placed into a quartz tube. Anodic polarization in the potentiostatic mode was carried out using a PI-50-1 potentiostat. Potentials were changed in 10-mV steps for 10–30 min until they acquired a constant current value.

After operations in melt were performed, a cooled salt melt was dissolved in distilled water; the precipitate was filtered and dried. The filtrate was analyzed on an Optima 4300 DV spectrometer. The surfaces of zirconium and tantalum samples after oxidation and the powders isolated from solution were studied with a Jeol SM 5900 LV scanning electron microscope, a Camebax electron probe microanalyzer, and a DRON-3 X-ray diffraction setup.

RESULTS AND DISCUSSION

Oxide synthesis is now carried out in two routes: to manufacture ultrathin films and ultrafine powders. Zirconium and tantalum metal samples are coated with oxide layers even during currentless exposure to cesium chloride + sodium chloride eutectic melts containing 10 wt % $NaNO_3$. The higher the nitrate ion concentration in the melt, the more rapidly metal corrosion

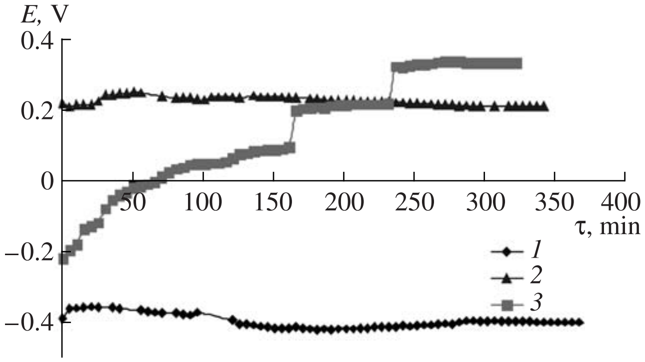

Fig. 1. Tantalum corrosion potentials vs. time in NaCl + CsCl + $NaNO_3$ melts containing (*1*) 0.10, (2) 10, and (*3*) 1 wt % $NaNO_3$ at T = 970 K.

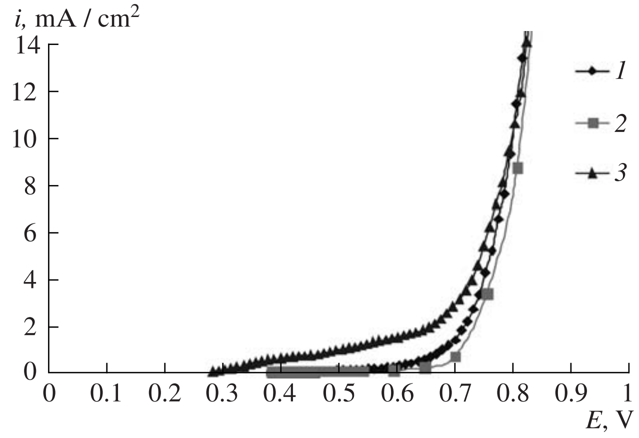

Fig. 2. Anodic polarization curves on tantalum in CsCl + NaCl + 10 wt % $NaNO_3$ melts at T = (*1*) 870, (2) 810, and (*3*) 970 K.

potentials are acquired. We relate this tendency to the appearance of oxide layers on the metal surface. For example, the tantalum corrosion potential in CsCl + NaCl melts containing 0.1–1.0 wt % $NaNO_3$ was acquired within 5 h; in the melt containing 10.0 wt %, within 2 h. A rise in the oxidation temperature shifts the tantalum potential toward positive values for all sodium nitrate additions. Interestingly, the acquisition of the corrosion potential at 970 K and 1.0 wt % $NaNO_3$ occurs in steps because of the poor adhesion of tantalum oxide flakes to the metal substrate: flakes at times fall into the melt (Fig. 1). At higher or lower sodium nitrite concentrations in chloride melts, the potential of oxidized tantalum is acquired more smoothly, without jumps, and reaches constant values more rapidly. The increasing sodium nitrate concentrations in the salt melt shift the corrosion potentials of the tantalum electrode into the anodic range (Table 1). There are indications of several potential plateaus, which systematically fall between the potential values for 0.1 and 10.0 wt % $NaNO_3$.

Anodic polarization curves for tantalum are passivation curves, with a passivation range of 300–400 mV and low passivation current densities (0.03–0.30 mA/cm^2) (Fig. 2).

The surface passivation of tantalum by solid corrosion products occurs even when the melt contains 0.1 wt % $NaNO_3$, producing thin (up to 1 μm thick) black layers of tantalum pentoxide. These films are very dense and keep tantalum from further dissolution. An increase in the sodium nitrate concentration leads to white loose deposits of tantalum oxide and sodium tantalate. Nitrate ions can reduce to various oxidation states (0, +2, or +4) in the reaction of tantalum with sodium (or cesium) nitrate, yielding tantalum oxide or tantalates. However, reactions with nitrogen or nitrogen oxide evolution are more likely; nitrogen dioxide almost is not expelled under steady-state conditions during exposure of tantalum and zirconium to chloride + nitrate melts.

We used X-ray powder diffraction and electron probe microanalysis to characterize the solid products of tantalum corrosion in NaCl + CsCl +$NaNO_3$ melts. We showed that the anodic polarization of tantalum at 810 K in melts containing $NaNO_3$ produces β-Ta_2O_5; when the oxidation temperature rises to 970 K, sodium tantalate (Na_2TaO_3) layers are formed. Ultrafine pow-

Table 1. Tantalum corrosion parameters in CsCl + NaCl + $NaNO_3$ melts

$NaNO_3$ wt %	T, K	E_{corr}, V	i_{corr}, A/cm^2	V, g/(cm^2 h)	i_{pass}, mA/cm^2
0.1	810	–0.407	4.6×10^{-5}	1.2×10^{-3}	0.28
	870	–0.455	8.7×10^{-5}	2.33×10^{-3}	0.4
	970	–0.263	6.3×10^{-5}	0.9×10^{-3}	0.24
1.0	810	–0.087	3.1×10^{-5}	2.0×10^{-3}	0.17
	870	0.420	0.7×10^{-5}	1.7×10^{-3}	0.10
	970	0.322	2.3×10^{-5}	2.7×10^{-3}	0.23
10.0	810	0.430	0.5×10^{-5}	0.49×10^{-2}	0.03
	870	0.434	1.3×10^{-5}	1×10^{-2}	0.16
	970	0.211	11×10^{-5}	0.14	0.9

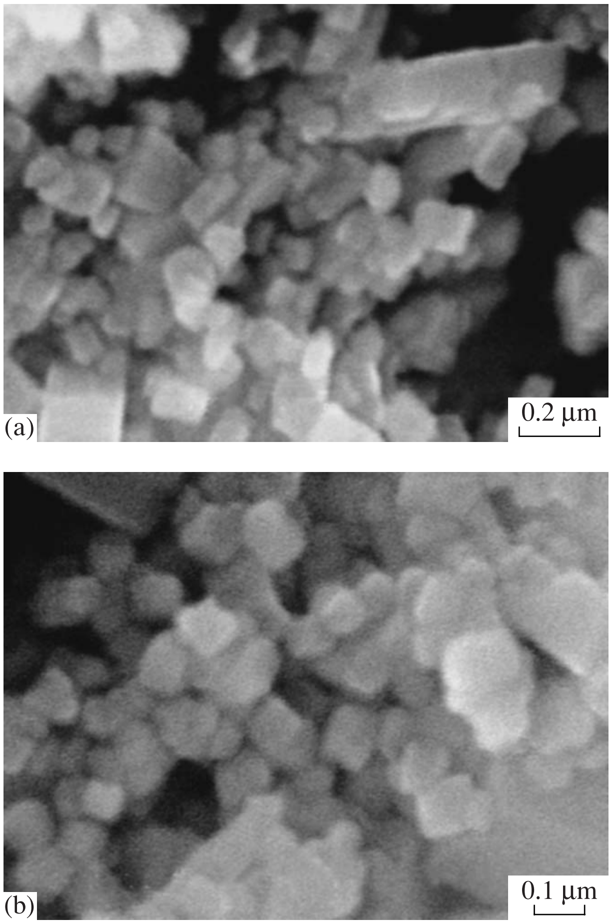

Fig. 3. Electron micrographs of a crystalline nanopowder after filtration from a cooled salt mass NaCl + CsCl + $NaNO_3$: (a) Ta_2O_5 and (b) $NaTaO_3$.

dered tantalum pentoxide falls into the melt (Fig. 3). The average particle size of powdered tantalum pentoxide is 50–100 nm. However, coarser crystals (up to 200 nm in size) exist; their fraction is not high. The tantalum oxide crystals prepared by anodic oxidation in chloride + nitrate melts are well faceted and have near-cubic shapes.

Inasmuch as tantalum oxide has a mixed conductivity, including oxygen-ion conductivity, the through oxidation of metal can be carried out under current to yield pure tantalum oxide (Fig. 4). The through tantalum oxidation is also made possible by the discontinuity of the oxide layer generated in an excess sodium nitrate; the layer consists of rather large oxide flakes, is defective, and cannot inhibit further penetration of oxygen to the metal.

The zirconium corrosion potentials in CsCl + NaCl + 1 wt % $NaNO_3$ melts also shift toward positive values as temperature rises, which is characteristic of an indifferent electrode. As the sodium nitrate concentration in the melt increases to 4.0–10.0 wt %, the potential shifts in the negative direction, as for a second-type electrode.

Figure 5 shows the zirconium potential as a function of oxidation temperature. When the chloride melt is doped by 1.0 wt % $NaNO_3$, the potential shifts in the positive direction with rising temperature because of the deposition of black dense zirconia layers with good adhesion to the metal substrate. The protective properties of these layers improve with rising deposition temperature. The corrosion potential is determined only by the activity of adsorbate oxygen on the metal surface at the oxygen partial pressure, which is controlled by the thermolysis of sodium nitrate; i.e., zirconium behaves as an indifferent electrode, which serves as an electron conductor and does not participate in the electrochemical process. Addition of 4.0 or 10.0 wt % to $NaNO_3$ the chloride melt shifts the corrosion potential toward negative values, probably because of the deposition of loose white oxide layers not adhering to the metal substrate. The oxide electrode potential is determined by the metal activity in the oxide phase [3].

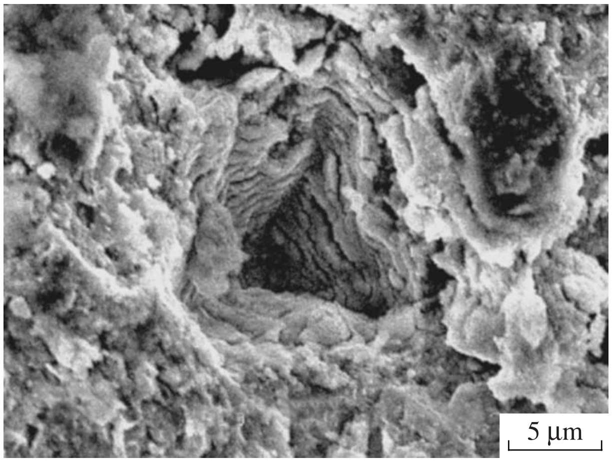

Fig. 4. Electron micrograph of a tantalum sample fully oxidized at 970 K.

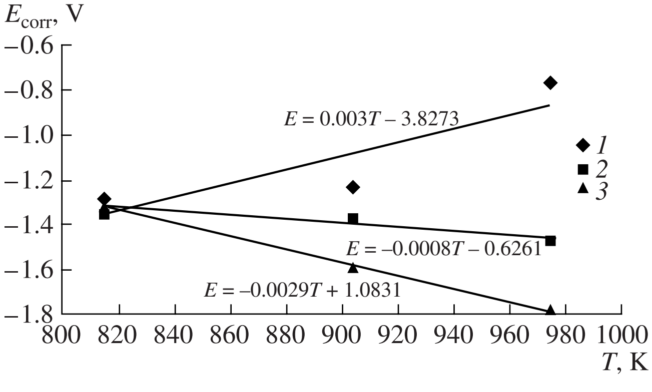

Fig. 5. Zirconium corrosion potential vs. temperature in CsCl + NaCl melts containing (*1*) 1, (*2*) 4, and (*3*) 10 wt % $NaNO_3$.

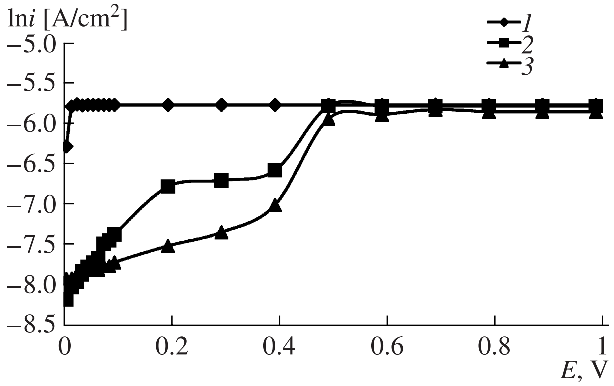

Fig. 6. Anodic polarization curves on zirconium in CsCl + NaCl eutectic melts containing (*1*) 1, (*2*) 4, and *3*) 10 wt % $NaNO_3$ at 903 K.

Chemical analysis does not show tantalum ions in the salt melt; all tantalum is firmly bound into the oxide film. At the same time, considerable amounts of nitrate ions are determined; e.g., in a melt containing 5 g $NaNO_3$ at 870 K, there is 0.110 g nitrate ions. The absence of tantalum ions in the salt melt is due to the oxide film on its surface; this was verified by X-ray powder diffraction and X-ray photoelectron spectroscopy.

Zirconium ion yields are rather considerable (up to 0.6 mg/(h cm^2)), probably because of an insufficient adhesion of the zirconia film to the metal substrate. Sodium or cesium zirconate formation was not observed because we recorded X-ray powder diffraction patterns after samples were washed with distilled water. This fact is explained as follows: the stability of zirconates decreases in the order Li_2ZrO_3–Na_2ZrO_3–$K_2Zr_3O_7$ [4].

The zirconium ion yield into the melt decreases substantially (about twofold) as the oxidation temperature in the CsCl + NaCl + 1.0 wt % $NaNO_3$ rises from 813 to 973 K; this agrees with our suggestion that a dense protective film is formed at high temperatures on the zirconium surface. This is also confirmed by gravimetric analysis, according to which the zirconium corrosion rate decreases by one order of magnitude in response to a 160-K rise in the oxidation temperature. The altered morphology (loosening) of the oxide film in response to the increase in the sodium nitrate concentration to 4.0 wt % indicates that the zirconium corrosion rate increases considerably (by one to two orders of magnitude), as made evident by gravimetric and chemical analyses. The oxide film formed in an excess of oxygen is not dense and does not keep nitrate ions from approaching the metal surface and zirconium under the oxide film from dissolving. The same is observed for addition of 10.0 wt % $NaNO_3$ to the melt (Table 2).

There are short anodic dissolution segments on the zirconium polarization curves; starting with potentials of +0.5 V, a constant current density equal to 3.10–3.45 mA/cm^2 is acquired (Fig. 6). The corrosion rate of a zirconium anode in the CsCl + NaCl + 1.0 wt % $NaNO_3$ eutectic melt calculated from anodic polarization curves decreases as the oxidation temperature rises from 813 to 973 K in agreement with gravimetric and chemical analysis data (Table 3). A further rise in temperature to 1023–1073 K gives a dramatic rise to the corrosion rate; we assign this rise to the appearance of pitting on the zirconium anode surface.

It is only at 903 and 973 K that the zirconium anodic polarization curve in the CsCl + NaCl + 10.0 wt % $NaNO_3$ is a passivation curve without an active dissolution segment and with the passivation current density

Table 2. Comparison of the results of chemical and gravimetric analyses

$NaNO_3$ wt %	*T*, K	Zr^{4+} concentration, %	NO_2^- concentration, %	V_{corr}, g/(cm^2 h)
1	813	0.03545	0.6575	5.355×10^{-3}
	903	0.021	1.08	-7.5×10^{-4}
	973	0.018	0.87	5.1×10^{-4}
4	813	–	0.53	5.9×10^{-3}
	903	0.25	1.54	3.8×10^{-2}
10	813	0.43	1.96	4.2×10^{-2}
	863	0.061	1.66	1.3×10^{-2}
	903	0.061	1.51	4.2×10^{-3}

Table 3. Corrosion and electrochemical parameters of zirconium in CsCl + NaCl + $NaNO_3$ melts

$NaNO_3$ wt %	*T*, K	E_{corr}, V	i_{corr}, A/cm^2	V_{corr}, g/(cm^2 h)
1	813	–1.376	5.815×10^{-3}	5.37×10^{-3}
	903	–1.279	34×10^{-3}	6.14×10^{-3}
	973	–0.784	4.5×10^{-3}	0.47×10^{-3}
	1023	–1.217	16.3×10^{-3}	-0.82×10^{-3}
	1073	–1.087	16.5×10^{-3}	1.56×10^{-3}
4	813	–1.288	0.585×10^{-3}	0.35×10^{-2}
	903	–1.341	1.02×10^{-3}	0.82×10^{-2}
	973	–1.467	2.1×10^{-3}	0.795×10^{-3}
10	813	–1.250	7.26×10^{-4}	1.87×10^{-2}
	863	–1.206	4.077×10^{-4}	4.18×10^{-2}
	903	–1.433	3.12×10^{-4}	0.86×10^{-2}
	973	–1.673	2.17×10^{-4}	-0.226×10^{-2}

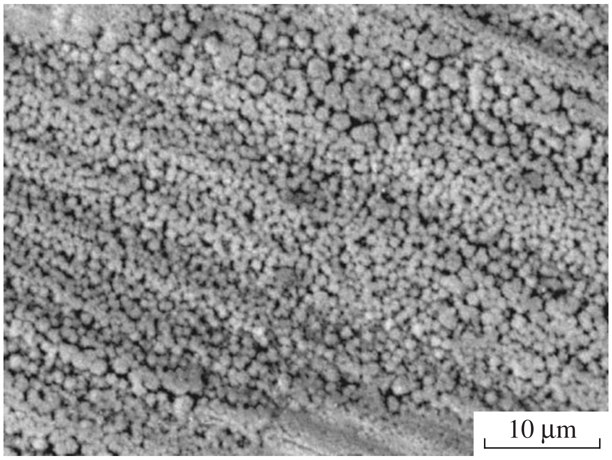

Fig. 7. Zirconium anode surface after 5-h exposure to a CsCl + NaCl eutectic + 1 % $NaNO_3$ melt at 810 K (black oxide).

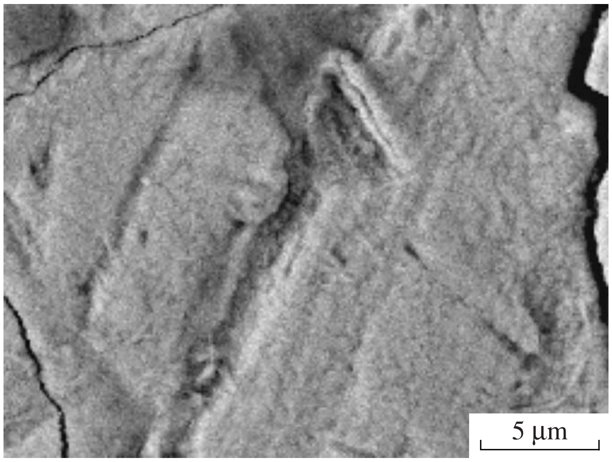

Fig. 8. Zirconium anode surface after 5-h exposure to a CsCl + NaCl eutectic + 10 % $NaNO_3$ melt at 870 K (white oxide).

equal to 0.55 and 0.17 mA/cm^2, respectively; the extent of the passivation plateau is 300 mV at 903 K and more than 1000 mV at 973 K. Anodic oxidation in the melt containing 4.0 or 10.0 wt % $NaNO_3$ at 973 K considerably shifts the potentials acquired after polarization toward positive values (200–300 mV). This can be due to the structural alterations that occur in the oxide at this temperature.

Zirconium oxidation yields oxide films of various colors, from black to white, with various corrosion properties.

Varied properties of oxide films are related to their deviation from the ZrO_2 stoichiometry. A white oxide film strictly corresponds to zirconium dioxide in its chemical composition; it loses protective properties during exposure to a greater degree than a black (oxygen-deficient) film. From this and because of the specifics of the anion-deficient structure of the oxide, a metastable ZrO_2 phase has a higher corrosion resistance. This oxide phase is nonstoichiometric zirconia. This phase coats the metal surface with a dense layer, insulating it from direct contact with the electrolyte, but does not interrupt the electrochemical reaction. An oxide phase with an anion-deficient structure and compositionally close to zirconium dioxide is a semiconductor, which has ionic and electronic conductivities [4].

Oxide layers capable of adsorbing oxygen from the gas space of the cell are formed on a zirconium electrode while it is exposed to a CsCl + NaCl + $NaNO_3$ melt until acquiring a steady state. During anodic polarization nitrite and nitrate ions discharge on the zirconium electrode coated with an oxide film:

$$NO_2^- - e \longrightarrow NO_2,$$
$$NO_3^- - e \longrightarrow NO_2 + \frac{1}{2}O_2.$$

Large amounts of grayish brown NO_2 gas are expelled during an experiment.

Removal of nitrite ions from the near-electrode layer enhances the appearance of dense, well adhering anodic oxide layers on the zirconium surface. Overlaying of the oxide film continues during the entire anodic polarization period.

Although the anodic polarization curves on zirconium are not typical passivation curves, the passivation currents established under all conditions are comparable to the values obtained during zirconium polarization in carbonate melts [5] but are one order of magnitude smaller than the zirconium passivation currents in chloride + peroxide melts [6]. However, there is a common tendency for zirconium oxidation in chloride + nitrate and chloride + hydroxide melts: passivation currents decrease as the oxidation temperature increases to 1073–1123 K; we assign this tendency to the formation of denser oxide layers with good adhesion. Zirconium oxidation in carbonate melts shows an opposite tendency.

Vigorous evolution of grayish brown nitrogen dioxide accompanies the anodic polarization of zirconium, Because the oxide layers deposited during the currentless exposure of zirconium to CsCl + NaCl + 4.0 (10.0) wt % $NaNO_3$ melts are loose and do not hinder the diffusion of oxygen ion O^{2-} through the oxide film, the zirconia formed on the metal surface can reach considerable thicknesses.

X-ray powder diffraction shows that the black layers (about 1 μm thick) generated by the reaction of zirconium with CsCl + NaCl eutectic + 1.0 wt % $NaNO_3$ melts are mixtures of tetragonal and monoclinic ZrO_2 (Fig. 7). Their black color indicates a possible off-stoichiometry (oxygen deficit) of zirconia. The white layers formed in CsCl + NaCl eutectic melts doped with 4.0 (10.0) wt % $NaNO_3$ consist of pure baddeleyite (*m*-ZrO_2) and have thicknesses of 0.07–0.12 μm (Fig. 8).

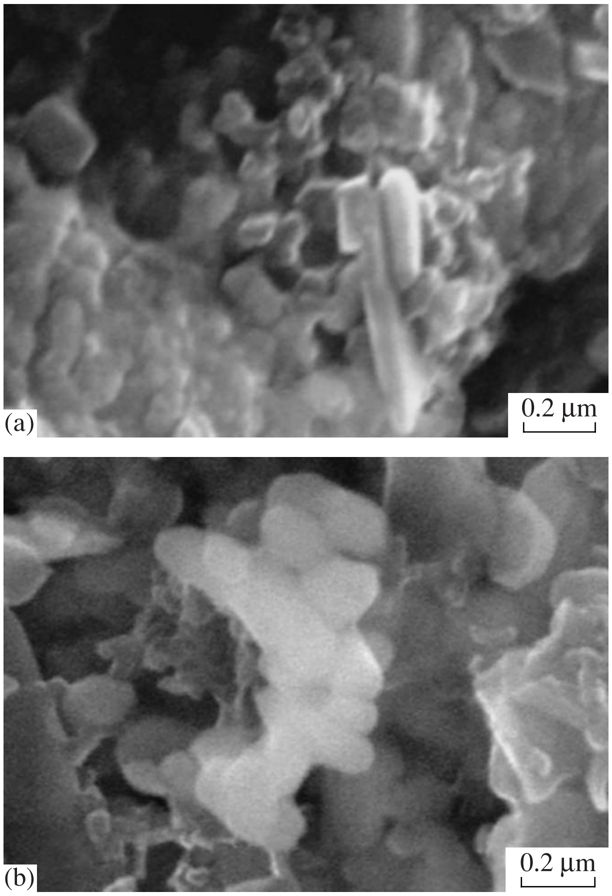

Fig. 9. Electron micrographs of zirconia powders filtered off a chloride + nitrate salt melt: (a) faceted crystals and (b) a column of large crystals.

The powder filtered after the fused salts dissolve is an ultramicrodisperse powder of monoclinic zirconia (Fig. 9). Zirconia grain sizes average 70–100 nm. Complex structures are noticed in the powder in the form of chains of large (100–200 nm) oval-shaped crystals.

Thus, the oxide film that appears in the initial moment of tantalum and zirconium oxidation in chloride + nitrate melts retards the process but does not interrupt ion exchange at the metal–melt interface. In the progress of oxide formation as the corrosion becomes a steady-state process, the oxidation rate is controlled by oxygen ion diffusion from the film surface into the bulk of the metal. Tantalum and zirconium oxidation yields oxide films of various colors (ranging from black to white), which have different corrosion properties.

The thinnest zirconia and tantalum pentoxide films, which have high protective properties, were obtained during anodic polarization of the metals. Considerable amounts of oxide powders with grain sizes from 50 to 200 nm can pile up in the melt.

To summarize, the oxidation of tantalum and zirconium in a molten eutectic mixture of cesium and sodium chlorides containing 0.1 to 30.0 wt % $NaNO_3$ is efficient for manufacturing thin films and nanopowders of tantalum pentoxide, sodium tantalate, and zirconia.

REFERENCES

1. P. Afanasiev and C. Geantet, Coord. Chem. Rev., Nos. 178–180, 1725 (1998).
2. E. G. Gillan and R. B. Kaner, J. Mater. Chem. **11**, 1951 (2001).
3. M. V. Smirnov, *Electrode Potentials in Molten Chlorides* (Nauka, Moscow, 1973) [in Russian].
4. B. G. Parfenov, V. V. Gerasimov, and G. I. Venediktova, *Corrosion of Zirconium and Its Alloys* (Atomizdat, Moscow, 1967) [in Russian].
5. T. I. Manukhina, I. N. Ozeryanaya, and B. D. Antonov, Zashch. Met., No. 2, 212 (1981).
6. I. N. Ozeryanaya, I. V. Zauzolkov, N. D. Shamanova, and M. V. Smirnov, Elektrokhim. Rasplavl. Sol. Tverd. Elektrol., No. 20, 90 (1973).